VOL. 11, NO. 21, NOVEMBER 2016 ISSN 1819-6608
ARPN Journal of Engineering and Applied Sciences

www.arpnjournals.com

PERFORMANCE ANALYSIS OFTHRESHOLDING TECHNIQUES ON WELD X-RADIOGRAPHY IMAGES

M. Muthukumaran, A. Sivapathi, L. Prabaharan and S. Gopalakrishnan
School of Computing, SASTRA University, Thanjavur, TN, India
E-Mail: mmkmtech@sastra.ac.in

ABSTRACT

Image thresholding is most important in image processing for unfolding foreground objects. In recent years, many thresholding methods have been proposed. However, identifying the weld defects on weld X-radiography images is a challenging task in Non-Destructive Testing (NDT) methods. Generally radiography images are in low contrast and lack of details. It is very difficult to extract the weld defects that are present. The main goal on this paper is to give comparative discussion on different threshold-based segmentation methods through performance measures. The thresholding techniques applied on various weld X-radiography images and their performance have been evaluated by non-uniformity (NU), misclassification error (ME) and relative foreground area error (RAE) measures. This performance analysis is supportive for an appropriate use of existing thresholding techniques on weld X-radiography image segmentation.

Keywords: image thresholding, thresholding technique evaluation, weld defects, weld x-radiography

1. INTRODUCTION

Weld defects are commonly arising for the duration of fault welding process. Inspection on the weldments is essential to ensure that the quality of the welds which in turn assures safety of the systems. Since the evaluation of weld defects is influenced by human's factor, human visual inspection is the basic evaluation method of many quality control programs. However more critical weld areas within the body of the weldment cannot be evaluated by humans and is also more subjective in nature. NDT methods can deliver efficient way for weld defect detection.

The challenges with respect to weld digital X-radiography image segmentation plays a key role in NDT methods. Each X-radiography image has different characteristics of contrast and visibility. So, it is difficult to segment X-radiography images using conventional image processing methods. One of the simplest and basic approaches to segment an image is based on the intensity levels that is threshold based approach. Therefore, thresholding techniques [1] [2] becomes a vital role for digital X-radiography image segmentation which are used to describe, analyze, cluster and classify an image.

The thresholding techniques categorize into six groups [1] which are: histogram shape, entropy, clustering, spatial, object attribute and the local based methods. In this paper we have discussed, three methods from cluster-based and entropy-based groups. The cluster-based methods based on the combination of Gaussian distributions and mean-square clustering. The following methods under the cluster-based group: Otsu (Clustering thresholding) [3], Kittler (Minimum error thresholding) [4] and Yanni's method [5]. The entropy-based algorithms deed the distribution entropy of the image gray levels. The following methods under the entropy-based: Kapur [6], Yen [7] and Pal [8].

2. THRESHOLDING TECHNIQUES

Otsu's cluster thresholding [3] is one of the most popular acceptable method to select the preferred threshold when the image histogram is bimodal distribution. It is based on the idea of finding an optimal threshold value that minimum value of sum of within-class variances derived from foreground and background pixels. Suppose an image f(x,y) contains a gray level range from 0 to L-1, where L is the gray levels. Let x_i indicates the total count of pixels at gray level i, and X denotes the total number of pixels in a given image with M × N size. The probability of gray level i is calculated as given below:

$$p_i = \frac{x_i}{X}, \quad \text{where } X = \sum_{i=1}^{L-1} x_i \tag{1}$$

If an image be separated into two classes $C_1(t)$ and $C_2(t)$, by threshold t. $C_1(t)$ class consist of pixels with levels [0,…,t] and $C_2(t)$ class consist of pixels with levels [t+1,…,L-1]. Let $p_1(t)$ and $p_2(t)$ denotes the cumulative probabilities, $\mu_1(t)$ and $\mu_2(t)$ denotes the mean of $C_1(t)$ and $C_2(t)$ classes respectively.

$$p_1(t) = \sum_{i=0}^{t} p_i \tag{2}$$

$$p_2(t) = \sum_{i=t+1}^{L-1} p_i = 1 - p_1(t) \tag{3}$$

The mean values of two classes can be calculated as

$$\mu_1(t) = \sum_{i=0}^{t} i \frac{p_i}{p_1(t)} \tag{4}$$

$$\mu_2(t) = \sum_{i=t+1}^{L-1} i \frac{p_i}{p_2(t)} \tag{5}$$

ARPN Journal of Engineering and Applied Sciences

and the individual class variances are given as

$$\sigma_1^2(t) = \sum_{i=0}^{t} (i - \mu_1(t))^2 \frac{p_i}{p_1(t)} \tag{6}$$

$$\sigma_2^2(t) = \sum_{i=t+1}^{L-1} (i - \mu_2(t))^2 \frac{p_i}{p_2(t)} \tag{7}$$

within-class variance, it can be calculated as

$$\sigma_w^2(t) = p_1(t)\sigma_1^2(t) + p_2(t)\sigma_2^2(t) \tag{8}$$

Thus, the optimal threshold t^* is calculated by minimizing the criterion function.

$$t^* = \underset{1 \le t < L}{\arg \min} \, \sigma_w^2(t) \tag{9}$$

Kittler's minimum error threshold [4] is based on combinationof distribution of foreground and background pixels. The minimum error threshold *t*can be computed by minimizing the criterion as

$$\begin{aligned} J(t) = 1 + 2[p_1(t)\log\sigma_1(t) + p_2(t)\log\sigma_2(t)] \\ - 2[p_1(t)\log p_1(t) + p_2(t)\log p_2(t)] \end{aligned} \tag{10}$$

Where σ_1 and σ_2 are standard deviation, and p_1 and $p_2$are priori probability.

Yanniand Horne [5] proposed that, the midpoint is employed in the mean of two peaks on the left and rightof the histogram that is

$$g_{mid}^* = (g_{peak1} + g_{peak2})/2 \tag{11}$$

The midpoint between peak1 and peak2 of the histogram can be calculated as

$$g_{mid} = (g_{\max} + g_{\min})/2 \tag{12}$$

Where $g_{\max}$ is the maximum non zero gray value and $g_{\min}$ is the minimum gray value.

The optimal threshold can be calculated as

$$T_{opt} = (g_{\max} - g_{\min}) \sum_{g=g_{\min}}^{g_{mid}^*} p(g) \tag{13}$$

Kapur *et al.* [6] method is an entropy based thresholding technique with different point of view. This method selects a threshold to divide the histogram intotwo probability distributions instead of one probability distribution. One probability distribution expressing the foreground and the other is for the background. The optimal threshold is selectedsuch that the sum of the each entropy of the foreground and the background is maximizing.

The probability distribution of the gray levels of the foreground and the background classes, η_1 and η_2, are given by

$$\eta_1 = \frac{p_0}{p(\eta_1)}, \frac{p_1}{p(\eta_1)}, \ldots, \frac{p_t}{p(\eta_1)} \tag{14}$$

$$\eta_2 = \frac{p_{t+1}}{p(\eta_2)}, \frac{p_{t+2}}{p(\eta_2)}, \ldots, \frac{p_{255}}{p(\eta_2)} \tag{15}$$

where

$$p(\eta_1) = \sum_{i=0}^{t} p_i, \; p(\eta_2) = \sum_{i=t+1}^{255} p_i \tag{16}$$

The foreground entropy is

$$K_f = -\sum_{i=0}^{t} \frac{p_i}{p(\eta_1)} \ln\left(\frac{p_i}{p(\eta_1)}\right) \tag{17}$$

and the background entropy is

$$K_b = -\sum_{i=t+1}^{255} \frac{p_i}{p(\eta_2)} \ln\left(\frac{p_i}{p(\eta_2)}\right) \tag{18}$$

The total entropy of the image is

$$K_T = K_f + K_b \tag{19}$$

The threshold T is selected as the one which maximizes K_T.

Yen et al. [7] defined the entropy correlation and selection of threshold that maximizes it. In this method, the correlation is used instead of entropy.

Definition: Let *Z* be a discrete random variable with finite or countably infinite range R={$x_0, x_1, x_2, \ldots$} and p_i denotes probability{Z=x_i}. The correlation *Z* is defined as

$$C(Z) = -\ln \sum_{i \ge 0} p_i^2 \tag{20}$$

Based on definition, the total amount of correlation provided by the distributions of foreground and background is

where

$$TC(s) = C_f(s) + C_b(s) \tag{21}$$

$$C_f(s) = -\ln \sum_{i=0}^{s-1} \left(\frac{p_i}{P(s)}\right)^2 \tag{22}$$

ARPN Journal of Engineering and Applied Sciences

$$C_b(s) = -\ln \sum_{i=s}^{m-1}\left(\frac{p_i}{1-P(s)}\right)^2 \tag{23}$$

The threshold s is selected as the one which maximizes TC(s).

An improved Minimum cross entropy [8] modeled the histogram by a combination of Poisson distribution and the threshold selected by minimizing the total cross entropy of the foreground and background feature space of an image.

The probability distribution of the foreground and background feature space are defined as

$$p_i^F = \frac{h_i}{P_s}, \quad i = 1,2,\ldots,s \tag{24}$$

$$p_i^B = \frac{h_i}{MN - P_s}, \quad i = s+1, s+2, \ldots L \tag{25}$$

where $P_s = \sum_{i=1}^{s} h_i$ and MN is the image size.

The Poisson distribution of the foreground and background gray value of the feature space is defined as

$$q_i^F = \frac{e^{-\lambda F}\lambda_F^i}{i!}, \quad i = 1,2,\ldots,s. \tag{26}$$

$$q_i^B = \frac{e^{-\lambda B}\lambda_B^i}{i!}, \quad i = s+1, s+2, \ldots, L. \tag{27}$$

where

$$\lambda_F = \left(\sum_{i=1}^{s} ih_i\right) \Big/ \sum_{i=1}^{s} h_i \tag{28}$$

$$\lambda_B = \left(\sum_{i=s+1}^{L} ih_i\right) \Big/ \sum_{i=s+1}^{L} h_i \tag{29}$$

The total cross entropy of the foreground and background region can be written as

$$D(s) = D_F(s) + D_B(s) \tag{30}$$

where

$$D_F(s) = \sum_{i=1}^{s} p_i^F \log\left(\frac{p_i^F}{q_i^F}\right) + \sum_{i=1}^{s} q_i^F \log\left(\frac{q_i^F}{p_i^F}\right) \tag{31}$$

$$D_B(s) = \sum_{i=s+1}^{L} p_i^B \log\left(\frac{p_i^B}{q_i^B}\right) + \sum_{i=s+1}^{L} q_i^B \log\left(\frac{q_i^B}{p_i^B}\right) \tag{32}$$

The threshold s is selected as the one which minimizing D(s).

3. EXPERIMENTAL RESULTS AND ANALYSIS

In this paper, we have implemented the above cluster-based and entropy-based methods which are Otsu's clustering thresholding [3], Kittler's minimum error threshold [4], Yanni's [5], Kapur's [6], Yen's [7] and Pal's[8] methods. The detailed comparisons are implemented in the weld X-radiography images.In order to evaluate the performance of these methods, metrics are employed on resultant images to evaluate the thresholding optimality. Ground truth image is used as reference image to measure the performance of various thresholding methods. Here, ground truth images have been created by manual threshold method on original image.

a) Region non-uniformity measure (NU) [1] does not require ground truth image, and is defined as

$$NU = \frac{|F_T|}{|F_T + B_T|}\frac{\sigma_f^2}{\sigma^2} \tag{33}$$

where σ_f^2 represents the foreground variance of the test image. σ^2 denotes the variance of the whole test image. F_T and B_T denote the foreground and background area pixels in the test image. Here, non-uniformity measure is close to 0 means well segmented image.

b) Misclassification error (ME) [1] for evaluation of the segmentation accuracy for a resultant image. It is relateto error ratio of background pixel that is determined as foreground and conversely. This metric requires ground truth image. Here, lower the value of ME contemplate as a better result. ME defined as follows:

$$ME = 1 - \frac{|B_o \cap B_T| + |F_o \cap F_T|}{|B_o| + |F_o|} \tag{34}$$

Where B_o and F_o represents the pixels from background and foreground area of the manually segmented image that is ground truth image respectively. B_T and F_T denotes the pixels from background and foreground area in the image that are segmented using various methods. |.| is the cardinality of the set.

c) Relative foreground area error (RAE) [1] is based on measure the segmented area and it can be calculate between segmented result and ground truth image. Here, lower the value of RAE contemplate as a better result. RAE is defined as:

$$RAE = \begin{cases} \dfrac{A_o - A_T}{A_o} & \text{if } A_T < A_o \\ \dfrac{A_T - A_o}{A_T} & \text{if } A_T \geq A_o \end{cases} \tag{35}$$

VOL. 11, NO. 21, NOVEMBER 2016 ISSN 1819-6608
ARPN Journal of Engineering and Applied Sciences

www.arpnjournals.com

Where A_o is foreground region of the manually segmented image that is ground truth image and A_T is foreground region of segmented resultant image.

In order to test the performance of above methods, a set of various weld X-radiography digital images with porosities, inclusions and crack defects are provided to be segmented. We examine the performance of the thresholding algorithms on: (1) Otsu, (2) Kittler, (3) Yanni, (4) Kapur, (5) Yen, and (6) Pal methods through NU, ME and RAE evaluation metrics. Figure 1- 2 shows segmentation results of six methods, illustrate histogram with threshold values and comparison chart of the average performance measure score of the resultant images. Table 1 lists the three evaluation measure values of the six methods. In which each listed method is tested for five weld images.

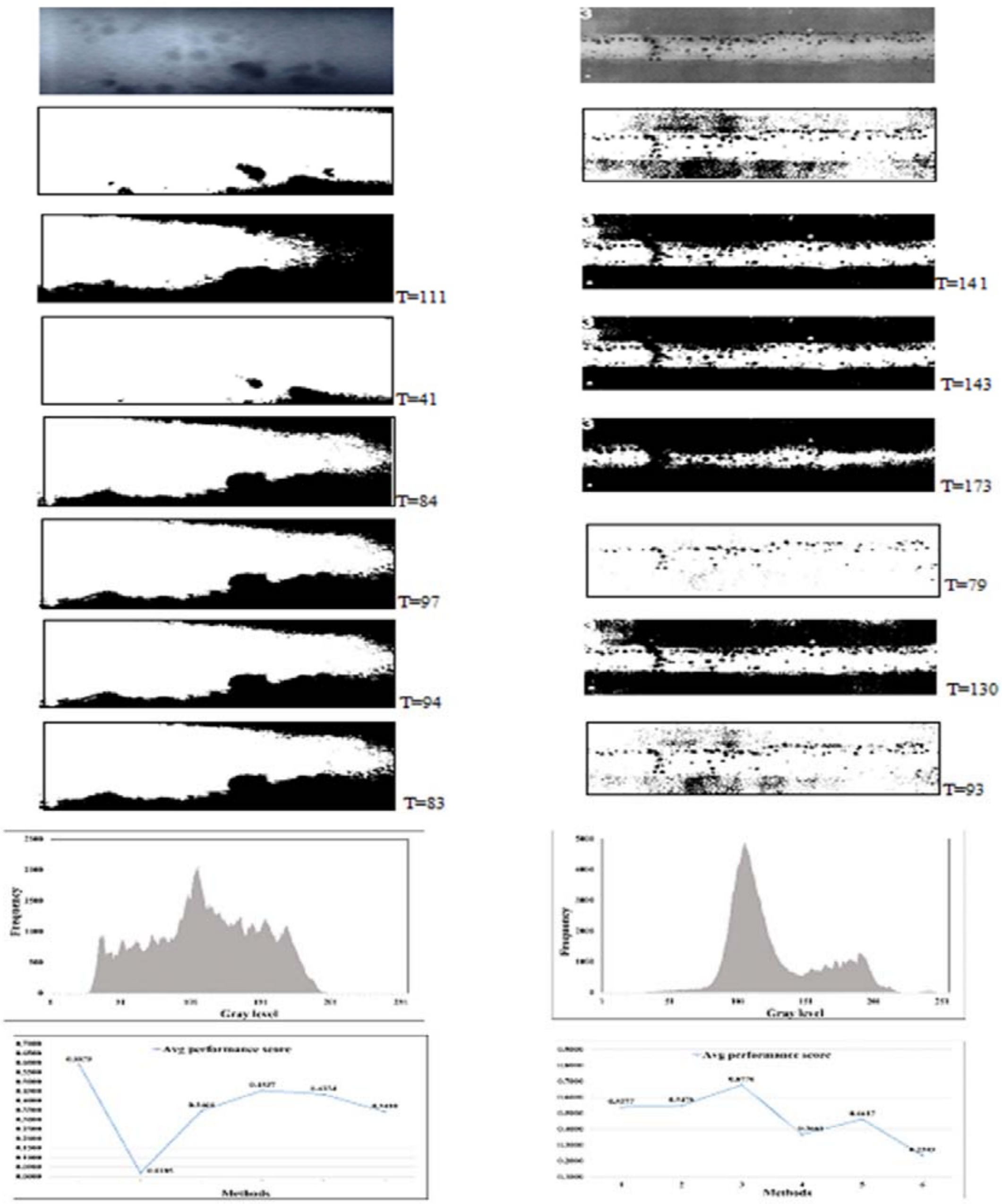

Figure-1. Segmentation results: First row: original weld image I and II; second row: ground truth image; from third to eighth row: segmentation results of the Otsu, Kittler, Yanni, Kapur, Yen and Pal method with threshold values; ninth row: histogram; tenth row: average performance score of the six methods derived from performance metrics.

VOL. 11, NO. 21, NOVEMBER 2016 ISSN 1819-6608
ARPN Journal of Engineering and Applied Sciences

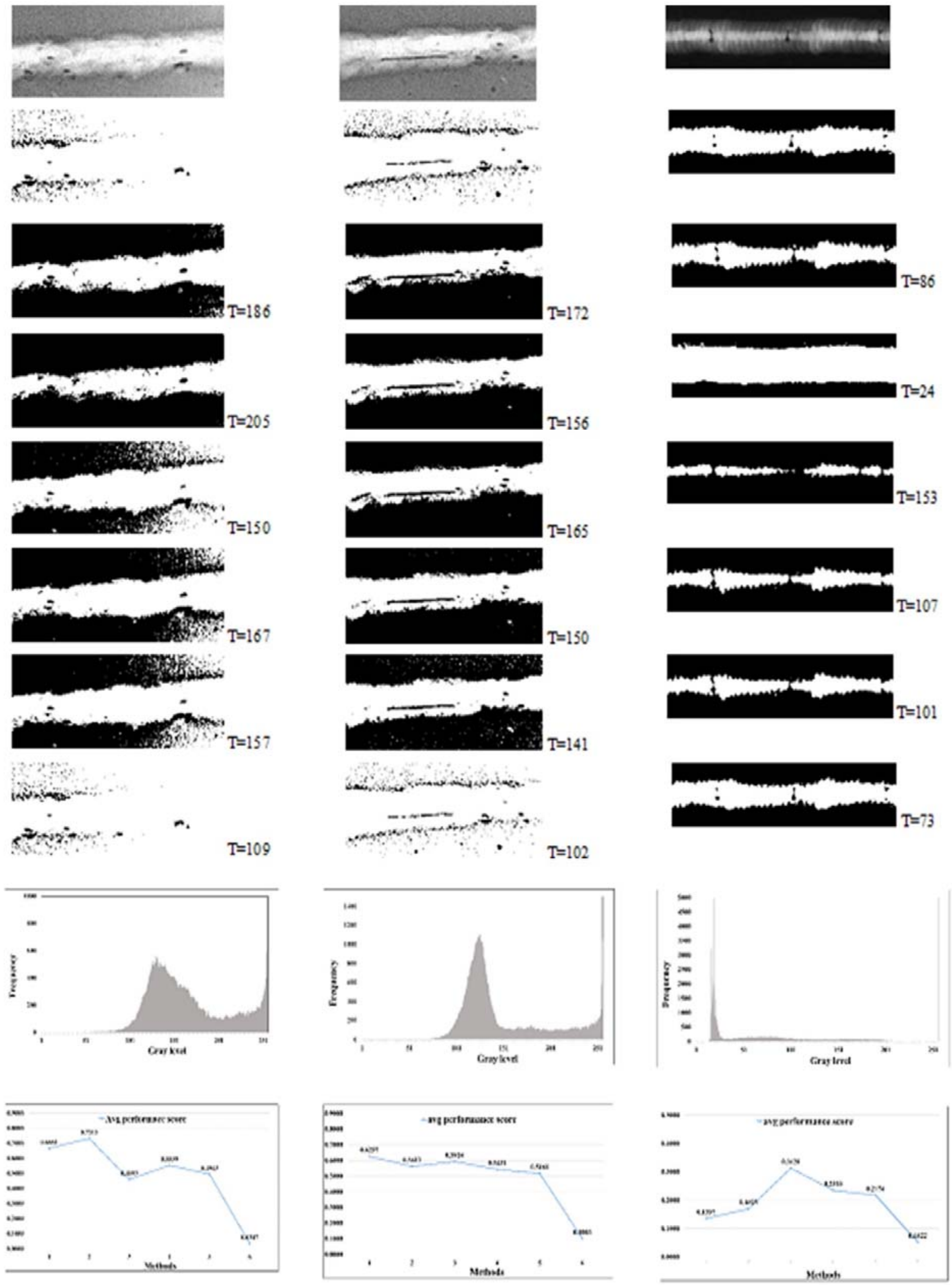

Figure-2. Segmentation results: First row: original weld image III, IV and V; second row: ground truth image; from third to eighth row: segmentation results of the Otsu, Kittler, Yanni, Kapur, Yen and Pal method with threshold values; ninth row: histogram; tenth row: average performance score of the six methods derived from performance metrics.

VOL. 11, NO. 21, NOVEMBER 2016 ISSN 1819-6608
ARPN Journal of Engineering and Applied Sciences

www.arpnjournals.com

Table-1. Performance evaluation measures of six methods on five weld images.

Origin images	Methods	NU	ME	RAE	Average performance score
Weld Image I	Otsu	0.3942	0.5284	0.8400	0.5875
	Kittler	0.0011	0.0052	0.0492	**0.0185**
	Yanni	0.0646	0.2565	0.7182	0.3464
	Kapur	0.1564	0.4042	0.8006	0.4537
	Yen	0.1422	0.3712	0.7867	0.4334
	Pal	0.0654	0.2470	0.7105	0.3410
Weld Image II	Otsu	0.3831	0.5173	0.7126	0.5377
	Kittler	0.4042	0.5236	0.7151	0.5476
	Yanni	0.6416	0.6378	0.7535	0.6776
	Kapur	0.0014	0.1893	0.9075	0.3661
	Yen	0.2187	0.4727	0.6938	0.4617
	Pal	0.0062	0.1203	0.5764	**0.2343**
Weld Image III	Otsu	0.4081	0.6537	0.9366	0.6661
	Kittler	0.5471	0.7064	0.9411	0.7315
	Yanni	0.0582	0.4159	0.9039	0.4593
	Kapur	0.1774	0.5579	0.9265	0.5539
	Yen	0.0895	0.4782	0.9153	0.4943
	Pal	0.0009	0.0044	0.0987	**0.0347**
Weld Image IV	Otsu	0.3174	0.6616	0.8982	0.6257
	Kittler	0.1725	0.6193	0.892	0.5613
	Yanni	0.2393	0.6424	0.8955	0.5924
	Kapur	0.1362	0.6037	0.8895	0.5431
	Yen	0.0908	0.5733	0.8843	0.5161
	Pal	0.0008	0.0209	0.2793	**0.1003**
Weld Image V	Otsu	0.2044	0.0852	0.1175	0.1357
	Kittler	0.0004	0.1982	0.3094	0.1693
	Yanni	0.4011	0.2536	0.2837	0.3128
	Kapur	0.3491	0.1585	0.1984	0.2353
	Yen	0.3292	0.1417	0.1812	0.2174
	Pal	0.1158	0.0162	0.0247	**0.0522**

4. CONCLUSIONS

This paper presented the various methods from cluster-based and entropy-based thresholding techniques to segment weld X-radiography images. There is also an attempt made to compare the results of six thresholding methods by their implementation. The optimum threshold value of the methods where obtained are evaluated by non-uniformity (NU), misclassification error (ME) and relative foreground area error (RAE) measures. From the measures as tried, we conclude that the Kittler's and Pal's methods are yield better results compared to other methods based on the average performance score. These thresholding techniques, in general, still require significant improvement to segment on weld X-radiography images. Therefore it is not possible to consider a single threshold method for weld X-radiography images nor all methods can perform well for a weld X-radiography image.

REFERENCES

[1] M. Sezgin and B. Sankur. 2004. Survey over Image Thresholding Techniques and Quantitative Performance Evaluation. Journal of Electronic Imaging. pp. 146-165.

 ISSN 1819-6608
ARPN Journal of Engineering and Applied Sciences

[2] N. Nacereddine, L. Hamami, D. Ziou. 2006. Thresholding Techniques and their Performance Evaluation for Weld Defect Detection in Radiographic Testing, Mach. Graph. Vis. 15(3/4): 557-566.

[3] N. Otsu. 1985. A threshold selection method from gray level histograms, IEEE Trans. Syst. Man Cybern. SMC-15, 652-655.

[4] J. Kittler and J. Illingworth. 1986. Minimum error thresholding, Pattern Recogn. 19, 41-47.

[5] M. K. Yanni and E. Horne. 1994. A new approach to dynamic thresholding, EUSIPCO'94: 9th European Conf. Sig. Process. 1, 34-44.

[6] J. N. Kapur, P. K. Sahoo, and A. K. C. Wong. 1985. A new method for gray-level picture thresholding using the entropy of the histogram, Graph Models Image Process. 29, 273-285.

[7] J. C. Yen, F. J. Chang and S. Chang. 1995. A new criterion for automatic multilevel thresholding,IEEE Trans. Image Process. IP-4, 370-378.

[8] N. R. Pal. 1996. On minimum cross-entropy thresholding, Pattern Recogn. 29(4): 575-580.